Mathematical Modelling and Analysis
Volume 14 Number 1, 2009, pages 109–126
Doi:10.3846/1392-6292.2009.14.109-126

ISSN 1392-6292 print
ISSN 1648-3510 online
www.vgtu.lt/mma/

Comparison of Finite-Difference Schemes for the Gross-Pitaevskii Equation

V. A. Trofimov and N. V. Peskov

Moscow State University
Faculty of Computational Mathematics and Cybernetics,
Moscow State University, Moscow, 119992 Russia

E-mail: vatro@cs.msu.ru

E-mail(*corresp.*): peskov@cs.msu.ru

Received September 23, 2008; revised January 16, 2009; published online February 25, 2009

Abstract. A conservative finite-difference scheme for numerical solution of the Gross-Pitaevskii equation is proposed. The scheme preserves three invariants of the problem: the L_2 norm of the solution, the impulse functional, and the energy functional. The advantages of the scheme are demonstrated via several numerical examples in comparison with some other well-known and widely used methods. The paper is organized as follows. In Section 2 we consider three main conservation laws of GPE and derive the evolution equations for first and second moments of a solution of GPE. In Section 3 we define the conservative finite-difference scheme and prove the discrete analogs of conservation laws. The remainder of Section 3 consists of a brief description of other finite-difference schemes, which will be compared with the conservative scheme. Section 4 presents the results of numerical solutions of three typical problems related to GPE, obtained by different methods. Comparison of the results confirms the advantages of conservative scheme. And finally we summarize our conclusions in Section 5.

Key words: Bose-Einstein condensate, Gross-Pitaevskii equation, conservative finite-difference scheme.

1 Introduction

Bose-Einstein condensate (BEC) is now an actual problem for a lot of theoretical and experimental studies. In the most cases the weakly interacting boson of the Gross-Pitaevskii theory has been invoked to describe the properties of BEC [11]. Nowadays, one of the most spectacular research is devoted to discuss the dynamics of BEC and the appearance of solitons [1, 5, 19, 20, 23, 30, 33, 37] based upon the Gross-Pitaevskii equation (GPE), which was derived independently by Gross [15, 16] and Pitaevskii [31]. Obviously, the GPE has many common features with the nonlinear Schrodinger equation (NSE) that is widely

investigated in connection with problems of laser physics (see, for example, [3, 4, 24]).

Owing to the active investigations of various aspects of BEC during the last years, GPE has been numerically treated by several methods. The comprehensive list of those methods with their specific features can be found in the review [28], for example, and in [2, 6, 29, 34]. It should be stressed that developing of finite-difference schemes for NSE attracts many authors in past twenty five years [7, 8, 9, 10, 12, 13, 14, 17, 25, 32, 39, 41, 43] and many other papers.

In general case, one can to distinguish two approaches to construction of numerical methods for NSE and GPE. First of them consists in splitting the equation into some parts, the number of final equations depends on the dimension and nonlinearity (and other factors) of the problem. In other words, a method of summary approximation is used to solve the equation. Let us notice, that this method in nonlinear optics is named usually as split-step method [14]. The advantage of this method is well-known. One can very easy to implement the computation procedure. But it has imperfection: this method preserves only one invariant (laser beam power) of NSE and its asymptotic stability is bad. It should be noticed, that the split-step method does not preserve the Hamilton function (the energy functional). In order to obtain good results on a long distance it is necessary to choose mesh steps in a definite way. Many authors have emphasized as well, that it is necessary to choose length of transverse domain so, that boundary values of be close to zero with a good accuracy. Only in this case the computation accuracy will satisfy the requiring conditions.

The second approach consists in designing the conservative finite-difference schemes for NSE (the review of application of this method to various problems of nonlinear optics are given in [22]). This approach allows one to get the preservation of all invariants for NSE. However conservative finite-difference schemes are nonlinear and require more arithmetic operations in comparison with the split-step methods. For many years the various papers deal with comparison of both classes of methods for NSE [17, 18, 26, 27, 28, 35, 36, 38, 40, 42]. It is proved that for weak nonlinearity (as the rule, the Kerr nonlinear response of medium) and for self-action of laser pulse and beam due to thermal blooming or Kerr effect, the split-step methods can have an advantages in speed of computation in comparison with conservative finite-difference schemes. But for soliton solution, high intense laser pulse propagation, or complicated nonlinear response of medium the advantages of conservative methods are obvious. We have got these results for SHG problem; propagation of laser pulse in nonlinear photonic crystals; propagation of laser femtosecond pulse in medium, which nonlinear response contains the time derivative of pulse; laser pulse interaction with semiconductor [26, 27, 36, 38, 40]. It should be noticed that for laser pulse propagation in the atmosphere with taking into account the turbulence, the big deviation of Hamiltonian from its initial value was shown in [18] where the split-step method was applied. The Hamiltonian deviation was up to 80%. For many problems of laser pulse interaction with matter such error is unacceptable.

Accounting of high interest to computer simulation of the BEC problems, it is of interest to compare conservative finite-difference scheme and split-step

methods for GPE. It is necessary to point out that the split-step method can be improved essentially if one uses an iteration procedure on the step of solution of nonlinear part of equations [42]. We consider below this method too. We demonstrate the advantages of the conservative finite-difference scheme for solving of GPE. The scheme preserves all three invariants at any size of the time and space step.

The paper is organized as follows. In Section 2 we consider ....

2 GPE and Conservation Laws

For simplicity, we will consider GPE in 1D space

$$\mathrm{i}\hbar\partial_t u(x,t) = \Big(-\frac{\hbar^2}{2m}\partial_{xx} + V(x,t) + g|u(x,t)|^2\Big)u(x,t),$$

where x is the space coordinate, $-\infty < x < \infty$; t is time, $t > 0$; $u(x,t)$ is the complex-valued macroscopic wave function in mean-field approximation; $V(x,t)$ is the real external potential; g is the real coupling constant ($g > 0$ for the repulsive interaction, and $g < 0$ for attractive interaction). In the following we accept the dimensionless units with the Plank constant $\hbar$=1 and the atomic mass m=1. We shall consider the initial-boundary value problem for GPE at the external potential $V(x,t) \equiv V(x)$ on the space-time domain $\Omega = \{-L \le x \le L,\ 0 \le t \le T\}$ in the form:

$$\begin{aligned} &\mathrm{i}\partial_t u(x,t) = \left(-\frac{1}{2}\partial_{xx} + V(x) + g|u(x,t)|^2\right) u(x,t); \qquad (2.1)\\ &u(x,t)\big|_{x=\pm L} = 0, \quad u(x,t)\big|_{t=0} = u_0(x). \end{aligned}$$

In order to consider the conservation laws, it is suitable to rewrite Eq. (2.1) in the form

$$\partial_t u(x,t) = -\mathrm{i}\hat{H}u(x,t), \quad \hat{H} = -\frac{1}{2}\partial_{xx} + V + g|u|^2,$$

where $\hat{H}$ is the Hamilton operator, which is symmetric in the Hilbert space of functions $u(x) \in L_2(-L,L)$ with zero boundary conditions.

There are three basic conservation laws for any solution of problem (2.1) and a violation of each of them in a numerical solution leads to incorrect evolution of $u(x,t)$.

1) The square of L_2 norm of solution is defined as

$$\mathcal{N}(t) = \int_{-L}^{L} |u(x,t)|^2\, dx. \qquad (2.2)$$

It is easy to see that due to symmetry of $\hat{H}$,

$$\frac{d}{dt}\mathcal{N}(t) = \int_{-L}^{L} (\partial_t u \cdot u^* + u \cdot \partial_t u^*)\, dx = \int_{-L}^{L} \left(-\mathrm{i}\hat{H}u \cdot u^* + u \cdot \mathrm{i}\hat{H}u^*\right) dx = 0,$$

where the u^* denotes the complex conjugation of u. Therefore we obtain that

$$\mathcal{N}(t) \equiv \mathcal{N}(0) = \text{const}.$$

In the theory of BEC the quantity $\mathcal{N}$ is interpreted as the number of atoms in BEC.

2) Let us consider the impulse functional ($\hat{p} = -\mathrm{i}\partial_x$ is the quantum mechanical impulse operator):

$$\mathcal{P}(t) = \int_{-L}^{L} u^*(x,t) \cdot (-\mathrm{i}\partial_x) u(x,t)\, dx = \frac{1}{2} \int_{-L}^{L} [u^* \cdot (-\mathrm{i}\partial_x u) + (-\mathrm{i}\partial_x u)^* \cdot u]\, dx. \tag{2.3}$$

Using the commutativity of operators ∂_t and ∂_x and the antisymmetry of ∂_x, one can obtain

$$\frac{d}{dt}\mathcal{P} = \mathrm{i} \int_{-L}^{L} (\partial_t u \cdot \partial_x u^* - \partial_t u^* \cdot \partial_x u)\, dx = -\frac{1}{2} \left[|\partial_x u|^2 \right]_{x=-L}^{x=L} - \int_{-L}^{L} \partial_x V \cdot |u|^2 dx. \tag{2.4}$$

In the following analysis we shall not take into account the boundary effects described by the first term on the right hand side of Eq. (2.4). Such assumption can be justified if the initial distribution $u_0(x)$ is finite and L is sufficiently large so that the solution $u(x,t)$ and its derivatives will be vanishing near the boundary points for all $t < T$.

The second term on the r.h.s. of the equality has the meaning of the average external force acting on the BEC and the equation is an analog of the second Newton law equation. For many applications the external potential V is the harmonic potential $V(x) = \frac{1}{2}kx^2$. In such a case Eq. (2.4) can be written as

$$\frac{d}{dt}\mathcal{P} = -kX_c, \quad X_c = \int_{-L}^{L} x|u|^2 dx,$$

where X_c is the average x-coordinate of BEC (the first moment of distribution function $|u|^2$).

Computing the first derivative of X_c with respect to t one could derive the equation defining the evolution of X_c:

$$\begin{aligned} \frac{d}{dt}X_c(t) &= \int_{-L}^{L} \left((\partial_t u^*) \cdot xu + u^* x \cdot (\partial_t u) \right) dx = \mathrm{i} \int_{-L}^{L} \left(xu \cdot \hat{H}u^* - x \cdot \hat{H}u \cdot u^* \right) dx \\ &= \mathrm{i} \int_{-L}^{L} \left(-\partial_x u \cdot u^* + x \cdot \hat{H}u \cdot u^* - x \cdot \hat{H}u \cdot u^* \right) dx = \mathcal{P}(t) \end{aligned}$$

Therefore,

$$\frac{d^2}{dt^2}X_c + kX_c = 0. \tag{2.5}$$

For $k > 0$ one obtains from Eq. (2.5)

$$X_c(t) = X_c(0)\cos(\sqrt{k}\,t) + (\mathcal{P}(0)/\sqrt{k})\sin(\sqrt{k}\,t). \tag{2.6}$$

Eq. (2.6) can be a useful additional benchmark for testing the numerical solution of problem (2.1).

3) The energy functional is defined as:

$$\begin{aligned}\mathcal{E}(t) &= \frac{1}{2}\int_{-L}^{L} u^*(x,t)\hat{H}u(x,t)\,dx \\ &= \frac{1}{2}\int_{-L}^{L}\left(\frac{1}{2}\left|\partial_x u(x,t)\right|^2 + V(x)\left|u(x,t)\right|^2 + \frac{1}{2}g\left|u(x,t)\right|^4\right)dx. \end{aligned} \tag{2.7}$$

Computing the derivative of $\mathcal{E}$ with respect to t we obtain:

$$\begin{aligned}\frac{d}{dt}\mathcal{E}(t) &= \frac{1}{2}\int_{-L}^{L}\left(\hat{H}u^*\cdot\partial_t u + \hat{H}u\cdot\partial_t u^*\right)dx \\ &= \frac{\mathrm{i}}{2}\int_{-L}^{L}\left(-\hat{H}u^*\cdot\hat{H}u + \hat{H}u\cdot\hat{H}u^*\right)dx = 0.\end{aligned}$$

Therefore, $\mathcal{E}(t) = \mathcal{E}(0) = \text{const}$. Let S_c denotes the second moment of the distribution $|u|^2$, i.e. $S_c = \int_{-L}^{L} x^2|u|^2\,dx$. Then one has

$$\frac{dS_c}{dt} = \mathrm{i}\int_{-L}^{L} x\left(u\partial_x u^* - u^*\partial_x u\right)dx,$$

and

$$\begin{aligned}\frac{d^2S_c}{dt^2} &= 2\int_{-L}^{L}|\partial_x u|^2\,dx - 2\int_{-L}^{L} x|u|^2\partial_x\left(V + g|u|^2\right)dx \\ &= 8\mathcal{E}(t) - 2\int_{-L}^{L}\left(2V + x\partial_x V\right)|u|^2\,dx - \int_{-L}^{L} g|u|^4\,dx.\end{aligned}$$

For the harmonic potential $V = \frac{1}{2}kx^2$ the following equation takes place

$$\frac{d^2S_c}{dt^2} + 4kS_c = 8\mathcal{E}(t) - \int_{-L}^{L} g|u|^4\,dx. \tag{2.8}$$

3 Finite-Difference Schemes

Let $\omega_x = \{x_j = jh,\ j = -M,\ldots,0,\ldots,M\}$ and $\omega_t = \{t_n = n\tau,\ n = 0,1,\ldots,N\}$ be a space and time grid with a space step $h = L/M$ and a time step $\tau = T/N$, and $\omega = \omega_x \times \omega_t$ is a grid in the domain Ω. Let us introduce a grid function $u_j^n = u(x_j,t_n)$ defined on ω. For the sake of brevity accept the following notations:

$$v_j = u_j^n,\ \ \hat{v}_j = u_j^{n+1},\ \ v_j^{0.5} = \left(\hat{v}_j + v_j\right)/2,$$

and standard notations for the time and space derivatives

$$v_{t,j} = (\hat{v}_j - v_j)/\tau,\ \ v_{x,j} = (v_{j+1} - v_j)/h,\ \ v_{\bar{x}x,j} = (v_{j-1} - 2v_j + v_{j+1})/h^2.$$

Below we present the conservative finite-difference scheme and some other schemes usually used to solve the NSE and GPE.

3.1 Conservative finite-difference scheme (CFDS)

For problem (2.1) we set the finite-difference problem

$$\begin{aligned} &\mathrm{i}v_{t,j} = -\frac{1}{2}v^{0.5}_{\bar{x}x,j} + \left[V_j + \frac{1}{2}g\left(|\hat{v}_j|^2 + |v_j|^2\right)\right] v^{0.5}_j,\ j = -M{+}1, \ldots, M{-}1, \\ &u^0_j = u_0(x_j),\ j = -M, \ldots, M, \\ &u^n_{-M} = u^n_M = 0,\ n = 0, 1, \ldots, N. \end{aligned} \tag{3.1}$$

In the linear case equation (3.1) is the well-known semi-implicit Crank – Nicholson scheme. In the nonlinear case this scheme is the conservative finite-difference scheme (CFDS) first proposed by Karamzin for nonlinear optics problems (see, for example, [21, 22]). This scheme reveals three nice features, it conserves the grid approximations of the norm (2.2), the impulse (2.3), and the energy (2.7).

For the generalized nonlinear Schrodinger equation

$$\mathrm{i}\partial_t u - \partial_{xx} u + Q'(|u|^2)u = 0,$$

with the energy functional

$$\frac{1}{2}\int_L^L \left[|\partial_x u(x,t)|^2 + Q(|u(x,t)|^2)\right]\, dx$$

the conservative finite-difference scheme

$$\mathrm{i}v_{t,j} = -\frac{1}{2}v^{0.5}_{\bar{x}x,j} + \frac{Q(|\hat{v}_j|^2) - Q(|v_j|^2)}{|\hat{v}_j|^2 - |v_j|^2} v^{0.5}_j \tag{3.2}$$

was proposed in [8, 12, 43]. The scheme (3.2) is equivalent to CFDS when applied to the GPE with $Q(s) = gs^2/2$. In application to the cubic nonlinear Schrodinger equation the scheme (3.2) was numerically studied in [7]. We stress, that there is a difficulty og realization of (3.2), when function in (3.2) is close to zero.

Let define the grid approximations of (2.2), (2.3), and (2.7) in the form:

$$\bar{\mathcal{N}} = \sum_{j=-M}^{j=M} |v_j|^2 h, \quad \bar{\mathcal{P}} = \sum_{j=-M}^{j=M-1} v^*_j \left(-\mathrm{i}v_{x,j}\right) h,$$

$$\bar{\mathcal{E}} = \frac{1}{2}\sum_{j=-M}^{j=M-1} \left(\frac{1}{2}\left|v_{x,j}\right|^2 + V_j\left|v_j\right|^2 + \frac{1}{2}g\left|v_j\right|^4\right) h.$$

Theorem 1. *If u^n_j, $j = -M+1, \ldots, M-1$ is the solution of* (3.1) *with initial data $u^0_j = u^0(x_j)$, $j = -M+1, \ldots, M-1$ and boundary conditions $u^n_{-M} = u^n_M = 0$, then for all n the following relations are valid*

$$\bar{\mathcal{N}}_t = 0;\ \ \bar{\mathcal{E}}_t = 0;\ \ \bar{\mathcal{P}}_t = -\sum_{j=-M}^{j=M-1} \left|v^{0.5}_j\right|^2 V_{x,j},$$

where the last equation is true when the boundary flux terms are also equal to zero.

Proof. One has

$$\bar{\mathcal{N}}_t = \frac{h}{\tau}\sum_{j=-M}^{j=M}\left(|\hat{v}_j|^2 - |v_j|^2\right) = h\sum_{j=-M}^{j=M}\left(\hat{v}_j v_{t,j}^* + v_j^* v_{t,j}\right).$$

Substituting in the r.h.s. the numerical time derivative from (3.1) one obtains

$$\bar{\mathcal{N}}^{n+1} - \bar{\mathcal{N}}^n = \mathrm{i}\tau h\sum_{j=-M+1}^{j=M-1}\Big\{-\hat{v}_j(v_{\bar{x}x,j}^{0.5})^* + \Big[V_j + \frac{g}{2}\left(|\hat{v}_j|^2 + |v_j|^2\right)\Big]\hat{v}_j\bar{v}_j^*$$

$$+ v_j^* v_{\bar{x}x,j}^{0.5} - \Big[V_j + \frac{g}{2}\left(|\hat{v}_j|^2 + |v_j|^2\right)\Big]\bar{v}_j v_j^*\Big\} = \mathrm{i}\frac{\tau h}{2}\sum_{j=-M+1}^{j=M-1}\Big\{\Big(\frac{1}{2}|\hat{v}_{x,j}|^2 + V_j|\hat{v}_j|^2$$

$$+ \frac{g}{2}|\hat{v}_j|^4\Big) - \Big(\frac{1}{2}|v_{x,j}|^2 + V_j|v_j|^2 + \frac{g}{2}|v_j|^4\Big)\Big\}.$$

Thus the following equality holds for the solution of Eq. (3.1)

$$\bar{\mathcal{N}}^{n+1} - \bar{\mathcal{N}}^n = \mathrm{i}\tau\left(\bar{\mathcal{E}}^{n+1} - \bar{\mathcal{E}}^n\right). \tag{3.3}$$

The norm $\bar{\mathcal{N}}^n$ and the energy $\bar{\mathcal{E}}^n$ are real numbers, hence Eq. (3.3) can be satisfied if and only if $\bar{\mathcal{N}}^{n+1} - \bar{\mathcal{N}}^n = 0$ and $\bar{\mathcal{E}}^{n+1} - \bar{\mathcal{E}}^n = 0$ for every n. Therefore, the quantities $\bar{\mathcal{N}}^n$ and $\bar{\mathcal{E}}^n$ are the invariants of Eq. (3.1), $\bar{\mathcal{N}}^n = \bar{\mathcal{N}}^0$, $\bar{\mathcal{E}}^n = \bar{\mathcal{E}}^0$.

For the discrete analog of impulse functional one has (for a case of zero derivatives at the domain boundary):

$$\bar{\mathcal{P}}_t = \sum_{j=-M+1}^{j=M}\mathrm{i}\left[v_{t,j}(v_{x,j}^{0.5})^* - v_{t,j}^* v_{x,j}^{0.5}\right]h = \sum_{j=-M+1}^{j=M}\Big[-\frac{1}{2}\left(v_{\bar{x}x,j}^{0.5}(v_{x,j}^{0.5})^* + v_{x,j}^{0.5}(v_{\bar{x}x,j}^{0.5})^*\right)$$

$$+ V_j\left((v_j^{0.5})^* v_{x,j}^{0.5} + v_j^{0.5}(v_{x,j}^{0.5})^*\right) + \frac{g}{2}\left(|\hat{v}_j|^2 + |v_j|^2\right)\left(v_j^{0.5}(v_{x,j}^{0.5})^* + (v_j^{0.5})^* v_{x,j}^{0.5}\right)\Big]h.$$

Summing by parts and omitting the boundary terms one obtains

$$\bar{\mathcal{P}}_t = -\sum_{j=-M+1}^{j=M}\left|v_j^{0.5}\right|^2 V_{x,j}.$$

The theorem is proved. □

Thus, the finite-difference equation (3.1) conserves the finite-difference analogs of the invariants for problem (2.1). The similar theorem is true for the general conservative scheme (3.2).

The equality $\bar{\mathcal{N}}^n = \bar{\mathcal{N}}^0$ reflects the unitarity of GPE and is a mandatory property of numerical solution of GPE. Practically all numerical methods applied to solve GPE possess this property. Meanwhile the second equality, $\bar{\mathcal{E}}^n = \bar{\mathcal{E}}^0$, is very important for accurate evolution of numerical solution, because it reflects the energy conservation in time-dependent GPE and defines correct evolution of the wave package phase. However, in the most numerical

methods the energy conservation property is absent. The choice of GPE nonlinear term approximation in CFDS gives the opportunity to preserve the norm and energy of numerical solution exactly. The accuracy of $\mathcal{N}$ and $\mathcal{E}$ preservation does not depend on time step τ and space step h, but only on the accuracy of solution of nonlinear equations (3.1) with respect to u^{n+1}.

The scheme (3.1) defines a system of $2M-1$ nonlinear algebraic equations with $2M-1$ unknown variables $\hat{v}_j$, which can be written in the form

$$F_j(v,\hat{v}) = L_j\hat{v} + f_j(v,\hat{v}) = 0,\ j = -M+1,\dots,M-1,$$

where L is the linear operator and f is the nonlinear function. We have solved this system by iterations

$$L_j\hat{v}^{(k+1)} + f_j(v,\hat{v}^{(k)}) = 0$$

with $\hat{v}^{(0)} = v$. The iterations converged if the following conditions are satisfied:

$$|\hat{v}_j^{(k+1)} - \hat{v}_j^{(k)}| < \varepsilon_1|\hat{v}_j^{(k)}| + \delta,\ \ j = -M+1,\dots,M-1.$$

In this paper we compare the CFDS with some other popular methods for numerical solving of GPE. Brief sketches of those methods are presented below.

3.2 Crank-Nicholson finite-difference method (CNFD)

It is the scheme the nonlinear term is taken from lower layer [34]:

$$\mathrm{i}v_{t,j} = -\frac{1}{2}v^{0.5}_{\bar{x}x,j} + \left(V_j + g\,|v_j|^2\right)v_j^{0.5},\quad j = -M+1,\dots,M-1, \quad (3.4)$$
$$u_j^0 = u_0(x_j),\ \ j = -M,\dots,M,\quad u^n_{-M} = u^n_M = 0,\ \ n = 0,1,\dots,N.$$

The scheme (3.4) differs from CFDS in the approximation of the nonlinear part of (2.1), here $|v|^2$ is taken from the previous time layer. This difference leads to breakdown of the energy and impulse conservation laws and causes of incorrect solution for long time intervals.

3.3 Split-step methods

Split-step methods are based on the approximation of solution for equation (2.1) in the form $u(t+\tau) \approx \exp[-\mathrm{i}\tau(\mathcal{L}+\mathcal{M}(u))]\cdot u(t)$, where $\mathcal{L} = -0.5\partial_{xx}$ and $\mathcal{M}(u) = V(x) + g|u|^2$, and further replacing the exponent of sum of operators by the product of exponents

$$\exp[-\mathrm{i}\tau(\mathcal{L}+\mathcal{M}(u))] \approx \exp[-\mathrm{i}\tau\mathcal{L}]\exp[-\mathrm{i}\tau\mathcal{M}(u)].$$

The last expression is exact whenever $\mathcal{L}$ and $\mathcal{M}$ commute and but otherwise it is only first order accurate. In practice the solution in the next time step is computed by the formula (the standard Strang [6] splitting)

$$u(t+\tau) \approx \exp[-0.5\mathrm{i}\tau\mathcal{M}(u)]\,\exp[-\mathrm{i}\tau\mathcal{L}]\,\exp[-0.5\mathrm{i}\tau\mathcal{M}(u)]\cdot u(t). \quad (3.5)$$

Thus in split-step method numerical solving of Eq. (2.1) is reduced to successive solving of two equations: linear one

$$\mathrm{i}\partial_t u = -\frac{1}{2}\partial_{xx} u, \tag{3.6}$$

and nonlinear one

$$\mathrm{i}\partial_t u = \left(V(x) + g|u|^2\right) u. \tag{3.7}$$

We consider three versions of the split-step method in application to the GPE.

3.3.1 Time-splitting spectral method (TSSP)

The TSSP method for solution of the GPE with periodic boundary conditions was proposed in [2]. It should be noticed that for nonlinear optic problems this method was proposed by Fleck at. al. in 1976 [13, 14].

In the TSSP method equation (3.6) is discretized in space by the Fourier spectral method and integrated in time exactly. Equation (3.7) leaves $|u|^2$ invariant in t and for $t \in [t_n, t_{n+1}]$ this equation can be replaced by

$$\mathrm{i}\partial_t u = \left(V + g|u^n|^2\right) u.$$

It changes only the phase of u and this equation can be integrated exactly

$$u^{n+1} = \exp\left[-\mathrm{i}\left(V(x) + g|u^n|^2\right)\tau\right] u^n.$$

The splitting steps are combined according to the equation (3.5):

$$\begin{aligned}
u_j^{(1)} &= \exp\left[-\mathrm{i}\frac{\tau}{2}\left(V_j + g|u_j^n|^2\right)\right] u_j^n,\\
u_j^{(2)} &= \frac{1}{M}\sum_{l=-M/2}^{M/2-1} \exp\left(-\mathrm{i}\mu_l^2\frac{\tau}{2}\right)\hat{u}_l^{(1)}\exp(\mathrm{i}\mu_l(x_j - L)),\\
u_j^{n+1} &= \exp\left[-\mathrm{i}\frac{\tau}{2}\left(V_j + g|u_j^{(2)}|^2\right)\right] u_j^{(2)},\ j = -M+1,\ldots,M-1,
\end{aligned}$$

where $\hat{u}_l^{(1)}$ are the Fourier coefficients of $u^{(1)}$ and they are defined as

$$\mu_l = \frac{\pi l}{L}, \quad \hat{u}_l^{(1)} = \sum_{j=-M+1}^{M-1} u_j^{(1)} \exp\left[-\mathrm{i}\mu_l(x_j - L)\right], \quad l = -\frac{M}{2},\ldots,\frac{M}{2} - 1.$$

We note that the TSSP method does not preserve the energy $\bar{\mathcal{E}}$.

3.3.2 Time-splitting spectral method with iterations (TSSI)

The GPE with periodic boundary conditions is also solved in two splitting steps. Like in TSSP one solves equation (3.6) by the Fourier spectral method (notice, that for 1D problems usage of the factorization algorithm to solve systems of linear equations is more preferable). But equation (3.7) is replaced with the Crank-Nicholson nonlinear finite-difference scheme

$$\mathrm{i}\,\frac{\hat{v}_j - v_j}{\tau} = V_j v_j^{0.5} + \frac{g}{2}\left(|\hat{v}_j|^2 + |v_j|^2\right) v_j^{0.5},$$

which is solved by an iteration method similar to CFDS.

The TSSI method does not preserve the energy $\bar{\mathcal{E}}$. But it allows one to control the energy with first order of accuracy in time. For problems of nonlinear optics this method was proposed in [42]. Its comparison with various finite-difference schemes (including conservative ones) was carried out in [26, 27, 36, 38, 40].

3.3.3 Time-splitting Runge-Kutta method (TSRK)

This method is widely used for solving of various problems of nonlinear optics (see, for example, references in [38]). In this method one solves the equation (3.6) for the time step τ by the Crank-Nicholson scheme

$$\mathrm{i}v_t = -v^{0.5}_{\bar{x}x}, \quad v_j = u^n_j. \tag{3.8}$$

Then one solves the nonlinear equation (3.7) by the Runge-Kutta method with the time step $\tau_1 = \tau/n$ (in our experiments we choose $n = 10$ and a second order Runge-Kutta method).

Note that for TSSI and TSRK methods there is no need to solve the GPE in the form (2.1) because in this case equation (3.7) is solved exactly. But in more general cases the potential V or the parameter g can be time dependent and the exact solution of (3.7) is not available. So we would like to consider these methods taking into account their wide usage for numerical solution of problems of nonlinear optics.

3.4 Modified Visscher method (VISS)

The starting point is to express the wave function as the sum of its real and imaginary parts, $u = A + \mathrm{i}B$ [39]. Then the evolution of each part is approximated by the relations:

$$A^{n+1}_j = A^{n-1}_j + 2H^n_{jk}B^n_k\tau, \quad B^{n+1}_j = B^{n-1}_j - 2H^n_{jk}A^n_k\tau$$

with the Euler-type start-up algorithm

$$A^1_j = A^0_j + 2H^0_{jk}B^0_k\tau, \quad B^1_j = B^0_j - 2H^0_{jk}A^0_k\tau.$$

Here H^n_{jk} is the discretized Hamiltonian and the repeating indexes define the sum. The Visscher method is conditionally stable and also does not preserve the energy integral.

4 Computer Simulation Results

Here we present three numerical examples demonstrating the advantages of CFDS in comparison with methods for solving of GPE listed in the previous section. First we solve the 1D initial-boundary problem (2.1) in the interval $(-L, L)$, $L = 32$, with the external potential $V(x) = \frac{1}{2}kx^2$, $k = 0.1$, the coupling constant $g = 1$, and the initial condition

$$u_0(x) = \frac{1}{(\pi\sigma^2)^{1/4}} \exp\left(-\frac{x^2}{2\sigma^2}\right), \tag{4.1}$$

where σ determines effective width of the initial distribution, $\sigma = 0.3$.

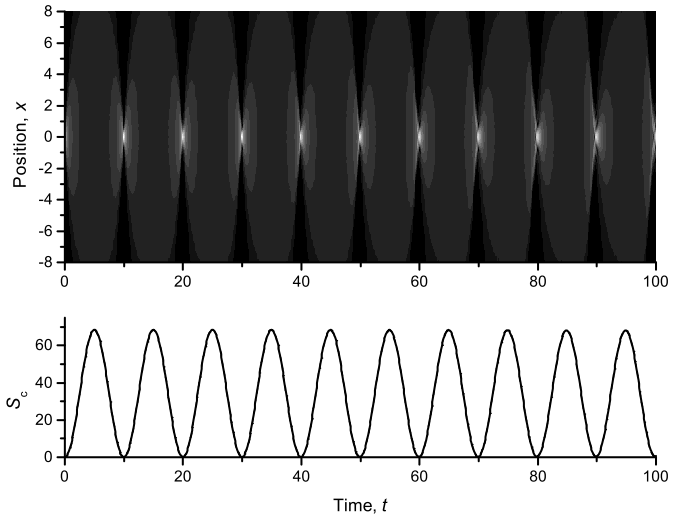

Figure 1. Upper panel: space-time plot $\left|u_j^n\right|$ of solution (3.1) at $\tau = 0.001$, $h = 1/128$. Bottom panel: the second moment of the distribution $|u|^2$ computed from the numerical solution and from Eq. (2.8), the two curves coincide in the scale of graph.

The upper panel of Fig. 1 shows a space-time plot of $\left|u_j^n\right|$ obtained using (3.1) with the time step $\tau = 0.001$ and the space step $h = 1/128$. The system of nonlinear equations (3.1) is solved by the method of simple iterations with the absolute accuracy $\varepsilon = 10^{-9}$, $\delta = 10^{-12}$. The bottom panel of Fig. 1 consists of the graphs of the second moment $S_c(t)$. They were obtained by numerical integration of the exact solution $x^2|u(x,t)|^2$ over the interval $-L \le x \le L$, and by numerical solution of (2.8). We see that both curves are indistinguishable in the graph's scale. Minimal values of S_c (minimal width of solution) coincide with maximal values of $|u|$, while maximal values of S_c correspond to widest spread of solution.

To compare solutions corresponding to different time steps we choose the numerical solution $U^{(0.0001)}$ obtained using $\tau = 0.0001$, $h = 1/64$, as a reference solution. Then we solve (3.1) using different values of τ and calculate the C and L_2 norms of difference $U^{(\tau)} - U^{(0.0001)}$. Fig. 2 presents the graphs of $\left\|U^\tau - U^{(0.0001)}\right\|_C$ and $\left\|U^\tau - U^{(0.0001)}\right\|_{L_2}$. We see that both norms of the difference $U^{(0.001)} - U^{(0.0001)}$ are less than 10^{-2} at $t < 100$ and their graphs almost coincide with t-axis.

The comparison of solutions obtained at different space steps are presented in Fig.2*b*. The solution $U_{(1/128)}$ obtained at $\tau = 0.001$ and $h = 1/128$ is considered as the reference solution. Two other solutions were obtained by using the same τ but different space steps $h = 1/64$ and $h = 1/32$. Here again the difference between the first pair of solutions $U_{(1/64)} - U_{(1/128)}$ is significantly smaller in comparison with the second pair $U_{(1/32)} - U_{(1/128)}$.

Thus, the numerical solution of (3.1) stabilizes readily enough for decreased

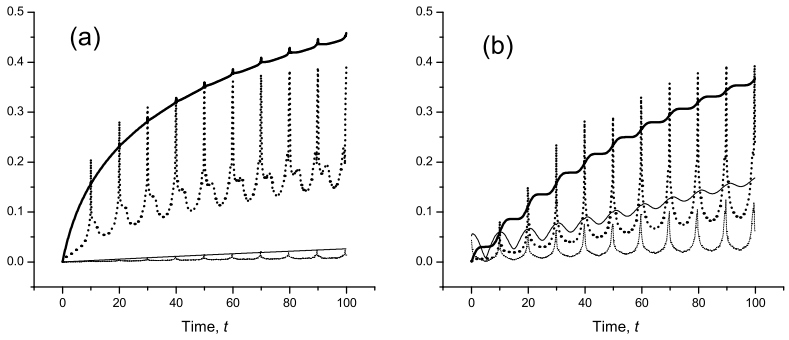

Figure 2. Comparison of solutions of (3.1) obtained by CFDS at (a) h=1/64 and τ0=0.0001, τ1=0.001, τ2=0.01, and (b) τ=0.001 and h0=1/128, h1=1/64, h2=1/32.

time and space steps, and the solution obtained at $\tau = 0.001$, $h = 1/64$ can be referred as a good approximation to the solution of problem (2.1). Comparing Fig.1 and Fig.2 one can see, that the main deviation of solutions takes place, when wave packet collapses to its minimum width. Obviously, this means that it is necessary to decrease a mesh step with respect space coordinate. This conclusion is clearly illustrated by Fig. 2.

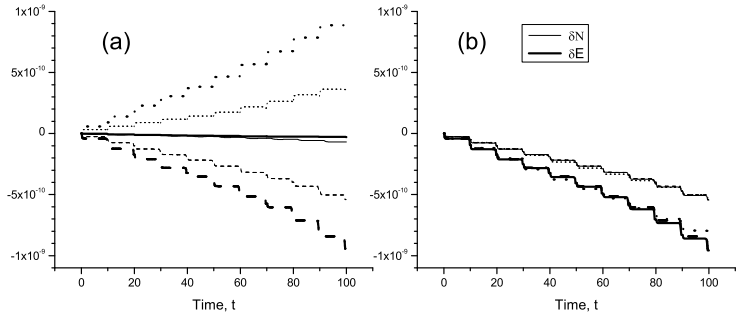

Figure 3. The dependence of relative deviations of invariants, $\delta\mathcal{N}$, and $\delta\mathcal{E}$ on time at different τ and h. (a) h=1/64, (b) τ=0.001.

Figure 3 shows the relative deviations of $\bar{\mathcal{N}}$, $\delta\bar{\mathcal{N}}$, $\bar{\mathcal{E}}$ and $\delta\bar{\mathcal{E}}$, calculated by the formula $\delta f(t) = (f(t) - f(0))/f(0)$ at different time and space steps. Note, that the deviation of $\mathcal{P}$ was zero for all these solutions, $\delta\bar{\mathcal{P}} \equiv 0$. One can see that the deviations of invariants do not depend on the space step h but depend on time step τ nonlinearly. At τ and h being fixed the deviations of invariants are determined by accuracy of solution of (3.1). For example, at τ=0.001, h=1/64, the maximal values of $\delta\bar{\mathcal{N}}$ and $\delta\bar{\mathcal{E}}$ in the interval $0 < t < 100$ for different values of ε are presented in Fig. 4.

Simultaneous preservation of the basic invariants of GPE is the key property

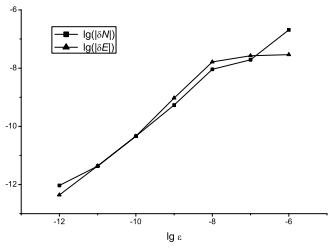

Figure 4. Logarithm of maximal deviations of invariants at $g = 1$, $k = 0.1$, for different values of ε.

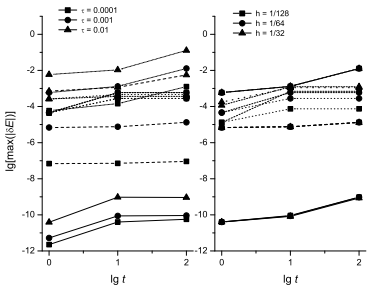

Figure 5. Logarithm of maximal deviations $\delta\bar{\mathcal{E}}$ at $g = 1$, $k = 0.1$, for different methods. (a) h=1/64, (b) τ=0.001.

of any efficient solver. Unfortunately, the most popular methods for solution of GPE do not possess such a property. For comparison we solved the problem (2.1) using the other methods listed in Section 3.

To compare preservation of invariants for GPE by these methods and CFDS we solved the problem (2.1) with the initial condition (4.1) in time interval $t \in [0, 100]$ and investigated the relative deviations of invariants. First, let us notice that under considered conditions the Visscher scheme is unstable and it is not considered below. The deviations $\delta\hat{\mathcal{N}}$ and $\delta\hat{\mathcal{P}}$ were very small ($< 10^{-9}$) in all computations and they are not presented here.

Fig. 5 shows the maximal deviations $\delta\bar{\mathcal{E}}$ for the solution of problem (2.1), (4.1) with $k = 0.1$, $g = 1$ in interval $t \in [0, 100]$, obtained with different numerical methods at different time and space steps. The presented data enables one to conclude that the best results in preservation of energy invariant can be got with the conservative scheme (3.1). While the preservation of invariants $\bar{\mathcal{N}}$ and $\bar{\mathcal{P}}$ is good enough in all methods, the $\bar{\mathcal{E}}$ preservation for scheme (3.1) is at least in five order of magnitude better than in other methods.This means that the latter methods can give incorrect solution if time t becomes large enough.

This fact can be easily observed by computing the well-known soliton solution of GPE with $V \equiv 0$. The energy changing during the time in non-conservative schemes leads to incorrect evolution of numerical solution. To illustrate this statement we give two numerical examples. The first example is concerned with famous nonlinear Schrodinger equation (NLS) with cubic nonlinearity, which in fact coincides with GPE at k=0 and g=−1. It is well known the NLS has the soliton solution of the form

$$u_s(x,t) = \frac{2\eta \exp\left(\mathrm{i}\eta^2 t/2\right)}{\exp\left(\eta x\right) + \exp\left(-\eta x\right)}. \tag{4.2}$$

We solved NLS with the initial data $u_j^0 = u_s(x_j, 0)$ by all listed above methods and computed the value of the mean square of the difference between

absolute values of the analytical solution (4.2) and numerical solution:

$$R(t_n) = \sum_{j=-M}^{M} \left(|u_j^n| - |u_s(x_j, t_n)|\right)^2 h, \quad n = 0, \ldots, N.$$

Parameters of numerical schemes were chosen as $L = 16$, $h = 1/128$, $\tau = 0.001$, and $\varepsilon = 10^{-9}$. At such values the best approximation is given by CFDS and CNFD, here the value of $R(t)$ is about 0.005. Very similar results of CFDS and CNFD in this case can be explain by the fact that the module of the exact soliton solution (4.2) does not depend on time.

All split-step methods produce insufficiently accurate solutions especially at large time interval. Fig. 6 present the mean square difference as a function of time for five numerical methods.

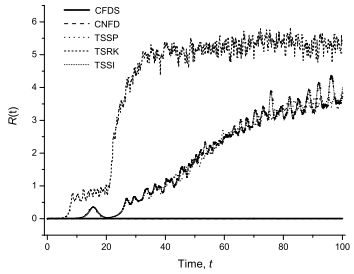

Figure 6. The mean square difference between the absolute values of the soliton solution $|u_s(x,t)|$ and numerical solutions $|u_j^n|$ of NLS obtained by different methods.

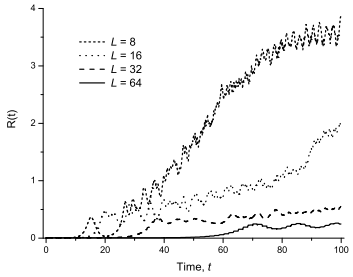

Figure 7. The mean square difference between the absolute values of the soliton solution $|u_s(x,t)|$ and the numerical solutions $|u_j^n|$ of NLS obtained by TSSP in the space intervals of different length.

The accuracy of solutions produced by time splitting methods is improved on a larger space intervals. For example, Fig. 7 presents the changes of the mean square difference between $|u_s|$ and solution obtained by TSSP with respect to the length L of the space interval $(-L, L)$. One can see that the larger is the space interval, the better approximation of solution is obtained. Therefore, TSSP needs much more larger space intervals than CFDS to obtain a solution that is comparable with CFDS solution in the accuracy of approximation.

The second example describes the GPE in self-focusing regime at g=−25 and k=0.1. We have solved the GPE at L=32, h=1/128, and τ=0.001 and investigated the change of average energy $\bar{\mathcal{E}}$ with respect to time.

The results of numerical experiments are shown in Fig. 8. One can see, that only CFDS scheme (3.1) is able to give a correct solution in this case ($|\delta\bar{\mathcal{E}}| < 10^{-6}$). The deviations of energy of non-conservative solutions are too large and the solutions can not be accepted as correct in the considered time interval.

A solution obtained by TSSP can be improved if one takes a longer interval L or a smaller value of τ. Fig. 9 shows the energy $\mathcal{E}$ of the solution of TSSP

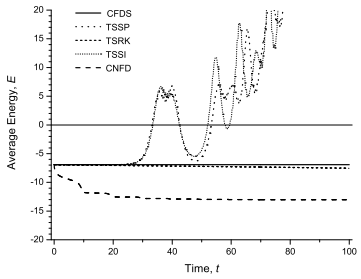

Figure 8. The energy of numerical solutions of GPE at $g = -25$ obtained by different methods.

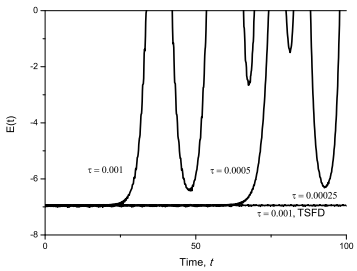

Figure 9. The deviation of energy in numerical solutions of the GPE at $g = -25$, obtained by TSSP for three values of τ.

corresponding to three values of time step: $\tau = 10^{-3}$ (the same as in Fig.8), $\tau = 5 \times 10^{-4}$ and $\tau = 2.5 \times 10^{-4}$. One can see, that for the last value of τ the numerical solution is valid on the whole interval $t < 100$.

Note that if we replace the spectral Fourier method of solution of Eq. (3.6) with finite-difference scheme (3.8), than the resulting method TSFD (time-split finite difference) is more robust for such type of problems. The energy of solution of TSFD obtained at $\tau = 0.001$ almost coincides with the energy of TSSP solution at $\tau = 2.5 \times 10^{-4}$ for $t < 100$.

5 Conclusions

We propose the conservative finite-difference scheme for solving of 1D GPE. The scheme preserves simultaneously the basic invariants of the GPE:

- the total number of particles $\mathcal{N}$,
- the impulse $\mathcal{P}$,
- the energy $\mathcal{E}$.

The comparison of efficiency of the proposed scheme with other modern numerical methods was made and the advantages of the conservative scheme were demonstrated. This scheme enables one to solve the GPE at such conditions when non-conservative schemes fail to give an adequate solution. The scheme can be easily generalized to multidimensional problems.

The numerical examples considered above demonstrate, that a seemed computational efficiency of the step-split method is vanished in the case of strong nonlinearity due to necessity of using smaller time steps or longer space intervals in order to achieve the same accuracy as CFDS.

6 Acknowledgments

The authors acknowledge the financial support from the Russian Fond of Basic Research, Grant 08-01-00107a.

References

[1] F.Kh. Abdullaev, A. Gammal, A.M. Kamchatnov and L. Tomio. Dynamics of bright matter wave solitons in a Bose-Einstein condensate. *Int. J. Mod. Phys. B*, **19**(22):3415–3473, 2005.

[2] S.K. Adhikari. Numerical study of the spherically symmetric Gross-Pitaevskii equation in two space dimensions. *Phys. Rev. E*, **62**(2):2937–2944, 2000.

[3] G.P. Agrawal. *Nonlinear fiber optics*. Academic Press, London, 1989.

[4] N.N. Akhmediev and A. Ankiewicz. *Solitons, Nonlinear Pulses and beams*. Chapman and Hall, London, 1997.

[5] R. Atre, P.K. Panigrahi and G.S. Agarwal. Class of solitary wave solutions of the one-dimensional Gross-Pitaevskii equation. *Phys. Rev. E*, **73**(5):056611, 2006.

[6] W. Bao, D. Jaksch and P. Markowich. Numerical solution of the Gross-Pitaevskii equation for Bose-Einstein condensation. *J. Comp. Phys.*, **187**(1):318–342, 2003.

[7] Q. Chang, E. Jia and W. Sun. Difference schemes for solving the generalized nonlinear schrodinger equation. *J. Comp. Phys.*, **148**(2):397–415, 1999.

[8] Q. Chang and L. Xu. A numerical method for a system of generalized nonlinear schrodinger equations. *J. Comput. Math.*, **4**(3):191–199, 1986.

[9] R. Čiegis. Completely conservative scheme for the problem of the interaction of three optical waves. *Lith. Math. J.*, **26**(4):389–393, 1986. (doi:10.1007/BF00971922)

[10] R. Čiegis. On the convergence in C norm of symmetric difference schemes for nonlinear evolution problems. *Lith. Math. J.*, **32**(2):147–161, 1992. (doi:10.1007/BF02450414)

[11] F. Dalfovo, S. Giorgini, L. P. Pitaevskii and S. Stringari. Theory of Bose-Einstein condensation in trapped gases. *Rev. Mod. Phys.*, **71**(3):463–512, 1999.

[12] M. Delfour, M. Fortin and G. Payre. Finite-difference solution of non-linear Schrodinger equation. *Comp. Math. Phys.*, **44**(2):277–288, 1981.

[13] M.D. Feit, J.A. Fleck and A. Steiger. Solution of the Schrodinger equation by a spectral method. *J. Comp. Phys.*, **47**(3):412–433, 1982.

[14] J.A. Fleck, J.R. Morris and M.D. Feit. Time-dependent propagation of high energy laser beams through the atmosphere. *Appl. Phys.*, **10**(2):129–160, 1976.

[15] E.P. Gross. Structure of a quantized vortex in boson systems. *Nuovo Cimento*, **20**(3):451–477, 1961.

[16] E.P. Gross. Hydrodynamics of a superfluid condensate. *J. Math. Phys.*, **4**(2):195–207, 1963.

[17] J. Hong, Y. Liu, H. Munthe-Kaas and A. Zanna. Globally conservative properties and error estimation of a multy-symplectic scheme for Schrodinger equation with variable coefficients. *Appl. Numer. Math.*, **56**(6):814–843, 2006.

[18] V.P. Kandidov and S.A. Shlenov. The laws of light field distribution propagating in the medium with cubic nonlinearity. *Bulletin of the Russian Academy of Sciences: Physics*, **50**(11):1191–1196, 1986.

[19] T. Kanna, M. Lakshmanan, P.T. Dinda and N. Akhmediev. Soliton collisions with shape change by intensity redistribution in mixed coupled nonlinear Schrodinger equations. *Phys. Rev. E*, **73**(2):026604, 2006.

[20] T. Kapitula, P.G. Kevrekidis and R. Carretero-Gonzalez. Rotating matter waves in Bose-Einstein condensates. *Physica D*, **233**(2):112–137, 2007.

[21] Yu.N. Karamzin. On finite-difference schemes for computing of three-frequencies interactions of electromagnetic waves in nonlinear medium with quadratic polarization. *Comp. Math. and Math. Phys.*, **14**(9):1058–1067, 1974.

[22] Yu.N. Karamzin, A.P. Sukhorukov and V. A. Trofimov. *Mathematical modeling in nonlinear optics*. Moscow University Press, 1989. (in Russian)

[23] Y.V. Kartashov, V.A. Vysloukh and L. Torner. Dynamics of surface solitons at the edge of chirped optical lattices. *Phys. Rev. A*, **76**(1):013831, 2007.

[24] Yu.S. Kivshar and D.E. Pelinovsky. Self-focusing and transverse instabilities of solitary waves. *Phys. Rep.*, **331**(4):117–195, 2000.

[25] L. Kong, R. Liu and X. Zheng. A survey on symplectic and multi-symplectic algorithms. *Appl. Math. Comput.*, **186**(1):670–684, 2007.

[26] M.M. Loginova and V.A. Trofimov. Difference scheme for the problem of femtosecond pulse interaction with semiconductor in the case of nonlinear mobility. *Comp. Math. and Math. Phys.*, **45**(12):2102–2112, 2005.

[27] M.M. Loginova and V.A. Trofimov. On the efficiency of some difference schemes for problems of nonlinear interaction of optical radiation with a semiconductor. *Diff. Equations*, **42**(8):1189–1198, 2006.

[28] A. Minguzzi, S. Succi, F. Toschi, M.P. Tosi and P. Vignolo. Numerical methods for atomic quantum gases with applications to Bose-Einstein condensates and to ultracold fermions. *Phys. Rep.*, **395**(4):223–355, 2004.

[29] P. Muruganandam and S.K. Adhikari. Bose-Einstein condensation dynamics in three dimensions by pseudo-spectral and finite-difference methods. *J. Phys. B*, **38**(12):2501–2514, 2003.

[30] G. Orso, C. Menotti and S. Stringari. Quantum fluctuations and collective oscillations of a Bose-Einstein condensate in a 2D optical lattice. *Phys. Rev. Lett.*, **97**(19):190408, 2006.

[31] L.P. Pitaevskii. Vortex lines in an imperfect Bose gas. *Sov. Phys. JETP*, **13**:451, 1961.

[32] J.M. Sanz-Serna and J.G. Verwer. Conservative and non-conservative schemes for the solution of the nonlinear Schrodinger equation. *IMA J. Numer. Anal.*, **6**(1):25–42, 1986.

[33] V.S. Shchesnovich, B.A. Malomed and R.A. Kraenkel. Solitons in Bose-Einstein condensates trapped in a double-well potential. *Physica D*, **188**(3):213–240, 2004.

[34] G. Strang. On the construction and comparison of differential schemes. *SIAM J. Numer. Anal.*, **5**(3):506–517, 1968.

[35] T.R. Taha and M.J. Ablowitz. Analytical and numerical aspects of certain nonlinear evolution equations. *J. Comp. Phys.*, **55**(2):203–230, 1984.

[36] E.B. Tereshin and V.A. Trofimov. Conservative difference schemes for the problem of propagation of a femtosecond pulse in a photonic crystal wiyh combined nonlinearity. *Comp. Math. Math. Phys.*, **46**(12):2154–2163, 2006.

[37] C. Trallero-Giner, J. Drake, V. Lopez-Richard, C. Trallero-Herrero and J.L. Birman. Bose-Einstein condensates: Analytical methods for the Gross-Pitaevskii equation. *Phys. Lett. A*, **354**(1):115–118, 2006.

[38] V.A. Trofimov and O.V. Matusevich. Comparison of efficiency of various difference schemes for the problem of SMG in media with quadratic and cubic nonlinear response, Finite difference methods: Theory and applications. In Farago I., Vabishchevich P. and Valkov L.(Eds.), *Proc. of Fourth Int. Conf. Lozenetz, Bulgaria, 2007*, pp. 320–325, 2007.

[39] P. Visscher. A fast explicit algorithm for the time-dependent Schrödinger equation. *Comp. Phys.*, **5**(6):596–598, 1991.

[40] A.G. Volkov, V.A. Trofimov and E.B. Tereshin. Conservative difference schemes for some problems of femtosecond optics. *Diff. Equations*, **41**(7):953–962, 2005.

[41] J.A. Weideman and B.M. Herbst. Split-step methods for the solution of the nonlinear Schrodinger equation. *SIAM J. Numer. Anal.*, **23**(3):485–507, 1986.

[42] I.G. Zakharova, Yu.N. Karamzin and V.A. Trofimov. *Split-step method in problems of nonlinear optics*. Keldysh Inst. Appl. Math., Moscow, 1989. (in Russian)

[43] F. Zhang, V.M. Perez-Garcia and L. Vazquez. Numerical simulation of nonlinear Schrodinger equation: A new conservative scheme. *Appl. Math. Comput.*, **71**(2–3):165–177, 1995.